Available online at www.sciencedirect.com
SCIENCE DIRECT
Polymer 46 (2005) 11442–11450
polymer
www.elsevier.com/locate/polymer

Characterization on mixed-crystal structure and properties of poly (butylene adipate-*co*-terephthalate) biodegradable fibers

X.Q. Shi, H. Ito, T. Kikutani *

Department of Organic and Polymeric Materials, Graduate School of Science and Engineering, Tokyo Institute of Technology, S8-32, 2-12-1, O-okayama, Meguro-ku, 152-8552 Tokyo, Japan

Received 20 May 2005; received in revised form 27 September 2005; accepted 12 October 2005

Abstract

Biodegradable ideal random copolymer poly(butylene adipate-*co*-terephthalate) (PBAT), with 44 mol% butylene terephthalate (BT), was melt-spun into fibers with take-up velocity up to 5 km/min. The structure development and properties of the as-spun fibers were investigated through birefringence, WAXD, SAXS, DSC and tensile test. Despite of the ideal randomness and composition (1:1) of PBAT copolymer, PBAT fiber showed well-developed PBT-like crystal structure, while its melting temperature (ca. 121 °C) was over 100 °C lower than that of PBT. Based on the quantitative analyses on the lattice spacing, the crystallinity and the fraction of crystallizable BT sequences, the crystal structure of PBAT was characterized to be formed by mixed-crystallization of BT and BA units, where BA units were incorporated into BT lattice. This mixed-crystal structure was found to undergo PBT-like reversible crystal modification with the application and removal of tensile stress. This crystal modification was found to occur in a higher strain region compared with that of PBT fibers.

Keywords: Poly(butylene adipate-*co*-terephthalate) (PBAT); Mixed-crystallization; Crystallizable sequences

1. Introduction

Biodegradable polymers currently achieve high interest in materials science since they are friendly to environment. Many biodegradable polymeric materials have been successfully developed and put into applications [1–8]. Among them, aliphatic/aromatic copolymers are an important series, because the balance of biodegradability (e.g. life time) and its physical properties (e.g. thermal and mechanical properties) can be adjusted by controlling the molar ratio of comonomers in these copolymers [9–17]. Poly(butylene adipate-*co*-terephthalate) (PBAT, Ecoflex®) is a commercialized aliphatic-*co*-aromatic biodegradable copolymer from BASF. Its biodegradation behavior and properties have been reported by Müller et al. [11,13,14,17]. PBAT was characterized to be an ideal random copolymer with 44 mol% of BT unit. It has been reported that the aliphatic/aromatic copolyester with aromatic units within the range of 35–55 mol% offers an optimal compromise of its biodegradability and physical properties [14,17]. Obviously polymer properties such as biodegradability, thermal property and mechanical property would also strongly depend on its crystal structure.

The crystal structure of PBAT has been reported by other groups [18,19]. However, based on their analyses on molecular mobility of the aliphatic methylene group in PBAT using solid-state ^{13}C NMR, their opinions diverge from each other on whether its crystal structure is formed by pure BT unit or by both BT and BA units.

By using solid-state ^{13}C NMR, our group have also reported the structure of a similar aliphatic–aromatic terpolymer, poly(butylene terephthalate-*co*-succinate-co-adipate), where its crystal structure was characterized to be formed by the mixed crystallization of its comonomers [20]. In addition, we found that the aliphatic methylene group is not suitable to be used to assign crystalline component in aliphatic/aromatic copolymers [20].

In this study, we attempt to characterize the crystal structure of PBAT from the view of crystallinity in weight (X_C) and the weight fraction of total crystallizable BT unit. The basic idea is that if we can verify that the X_C is larger than the weight fraction of crystallizable BT unit, then undoubtedly the crystal structure of PBAT should be formed by both BT and BA units.

In addition, there are increasing demands of biodegradable fibers in both agricultural and medical fields, however all

* Corresponding author. Fax: +81 3 5734 2876.
E-mail address: tkikutan@o.cc.titech.ac.jp (T. Kikutani).

0032-3861/$ - see front matter © 2005 Elsevier Ltd. All rights reserved.
doi:10.1016/j.polymer.2005.10.065

the studies on PBAT till now are based on film samples. Thus this study is also expected to yield information on biodegradable fiber processing and resultant fiber properties.

2. Experimental

2.1. Materials and as-spun fibers preparation

PBAT copolymer pellets were kindly supplied by BASF, Japan. Fig. 1 shows the chemical structure of PBAT. The pellets were dried at 60 °C for 12 h before melt spinning to avoid the possible hydrolysis during extrusion process. The polymer was extruded from a single-hole spinneret of 1 mm diameter at 220 °C. The throughput rate was controlled at 5.0 g/min. As-spun fiber was taken-up by a high-speed winder placed at 330 cm below the spinneret. PBAT copolymer showed fairly good spinnability, and the maximum take-up velocity of 5 km/min was attained. For comparison, PBT fibers, being extruded at 260 °C and prepared at 5 km/min, were used as reference sample in this work.

2.2. Birefringence measurement

Refractive indices parallel and perpendicular to the fiber axis, $n_{\parallel}$ and $n_{\perp}$, were measured using an interference microscope (Carl Zesis Jena). Birefringence Δn was calculated using Eq. (1):

$$\Delta n = n_{\parallel} - n_{\perp} \tag{1}$$

2.3. Differential scanning calorimetry (DSC)

The melting temperature (T_m) of PBAT fiber was analyzed by using a differential scanning calorimeter (Rigaku DSC 8230). About 5 mg of PBAT fiber sample was cut into powder shape and encapsulated in aluminum DSC pan. The DSC measurement was carried out from room temperature to 250 °C at a heating rate of 10 °C/min. For comparison, measurement on poly(butylene terephthalate) (PBT) fiber was also conducted.

In addition to T_m, the equilibrium melting temperature of PBAT was determined by using Hoffman-Weeks plot [21]. About 5 mg of PBAT powder sample, encapsulated in DSC pan, was held at 170 °C in a vacuum dryer for 30 min to eliminate sample thermal history. The sample was then transferred to DSC within seconds, where DSC was preset at a given crystallization temperature (T_C) for 30 min. The sample was held at T_C for equilibrium crystallization for 1 h. After the crystallization, the temperature was increased to 160 °C at a heating rate of 10 °C/min. The corresponding melting temperature for each T_C was investigated.

2.4. Tensile test

The stress–strain curves of the fiber samples were obtained using a tensile tester (Toyosokki, UTM-4L). The gauge length was 20 mm and the tensile speed was 20 mm/min. A representative stress–strain curve was determined by at least 10 trials of the test for each kind of fiber.

2.5. Wide-angle X-ray diffraction (WAXD) measurement

Wide-angle X-ray diffraction (WAXD) patterns of the fiber bundle were obtained by using an X-ray generator (Rigaku Denki) and a charge-coupled device (CCD) detector. The generator was operated at 40 kV and 300 mA with a monochromatized CuKα radiation. The camera length, which is the distance between the sample and CCD, was 45.5 mm, and the exposure time was 25 s.

In the case of uniaxial oriented fiber samples, and when the diffraction intensity is recorded by a flat CCD camera, the degree of crystallinity in weight (X_c) can be estimated by using Eq. (2). The crystalline orientation can be determined quantitatively by computation of the Hermans orientation factor [22]. This orientation factor $f_{(c,\ z)}$ of PBAT fibers was estimated by using Eqs. (3)–(5). In addition, the crystallite size of PBAT fibers was estimated according to Scherrer equation [23].

$$X_c = \frac{\int_{2\theta_1}^{2\theta_2} \cos\theta \int_0^{\pi/2} I_c(\delta,\theta)\sin\delta d\delta d(2\theta)}{\int_{2\theta_1}^{2\theta_2} \cos\theta \int_0^{\pi/2} I(\delta,\theta)\sin\delta d\delta d(2\theta)} \tag{2}$$

$$\langle\cos^2\phi_{010,z}\rangle = \frac{\int_0^{\pi/2} I(\delta)_{010}\cos^2\theta\cos^2\delta\sin\delta d\delta}{\int_0^{\pi/2} I(\delta)_{010}\sin\delta d\delta} \tag{3}$$

$$\langle\cos^2\phi_{c,z}\rangle = 1 - 2\langle\cos^2\phi_{010,z}\rangle \tag{4}$$

$$f_{(c,z)} = \frac{3\langle\cos^2\phi_{c,z}\rangle - 1}{2} = 1 - 3\langle\cos^2\phi_{010,z}\rangle \tag{5}$$

where, θ is Bragg angle, in this work, $2\theta_1 = 5°$, and $2\theta_2 = 40°$; ϕ is azimuthal angle, the angle between the normal of crystal plane and fiber orientation axis; and $\delta$is the azimuthal angle

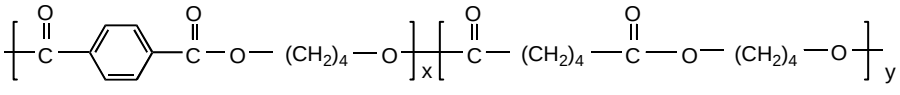

Fig. 1. Chemical structure of poly(butylene adipate-*co*-terephthalate).

from the meridian in WAXD pattern recorded by flat CCD camera.

In addition to the conventional WAXD measurement, in situ WAXD measurement during tensile deformation was performed to investigate the crystal form transition of PBAT fiber. A mini tensile testing machine (Kyowa) was used to impose the tensile deformation. The tensile machine allowed symmetric deformation of the sample, which permitted the focused X-ray to illuminate the same sample position during stretching. About 1500 filaments of PBAT fibers, prepared at the take-up velocity of 5 km/min with the diameter of 34 μm, were aligned parallel to each other at a width of 8 mm to obtain sufficient diffraction intensity. The camera length was 45.0 mm and the exposure time was 10 s. The gauge length was 20 mm. The tensile deformation was carried out in creep mode. A series of WAXD patterns were recorded with the increase of tensile load. Reflections close to the meridional direction were clearly monitored by tilting the fiber bundle properly in a plane containing the X-ray beam and the fiber bundle.

2.6. Small-angle X-ray scattering (SAXS)

Small-angle X-ray scattering (SAXS) was performed by using NANO-Viewer system (Rigaku Co., Japan). A CuKα radiation (40 kV, 20 mA) was generated by RA-Micro7 (Rigaku Co.) and concentrated by Confocal MAX-Flux® (CMF) optic, which acts as a monochromator ($\lambda = 0.154$ nm). The X-ray beam was collimated by pin-holes; the sizes of 1st, 2nd, and 3rd pin-holes were ϕ0.4, ϕ0.2, and ϕ0.45 mm, respectively. An imaging plate (IP) (Fujifilm BAS-SR 127) was used as a two dimensional detector and the resolution (pixel size) was set to 50 μm in an IP reading device (R-AXIS D3, Rigaku Co.). The pin-holes, sample, and IP film were set in a vacuum chamber and the two-dimensional scattering pattern was measured under a vacuum, which eliminates air scattering. The camera length was 482 mm, and the exposure time was set to 120 min.

3. Results and discussion

3.1. Characterization on as-spun fibers

3.1.1. Birefringence

Birefringence of PBAT fibers was increased with increasing take-up velocity as shown in Fig. 2. It indicates the molecular orientation was enhanced by higher spinning line stress induced by higher take-up velocity. It is notable that PBAT fibers prepared even at low take-up velocity show a fairly high birefringence. This may be attributed to the presence of the benzene ring in PBAT, which yields high intrinsic birefringence and high molecular rigidity.

3.1.2. WAXD patterns

WAXD patterns of PBAT fibers with different take-up velocities are shown in Fig. 3. Diffraction spots became more distinct with increasing take-up velocity. The sharp diffraction spots indicate that PBAT fibers have well-developed

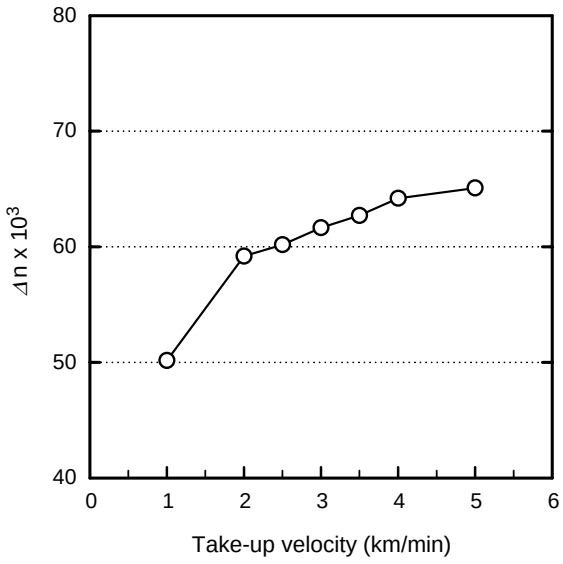

Fig. 2. Birefringence of PBAT fibers as a function of take-up velocity.

and highly oriented crystal structure. Quantitative evaluation on the crystal structure of PBAT fibers in terms of crystalline orientation, crystallinity, and crystallite size will be given below.

3.1.3. Melting temperature

PBAT fibers showed similar DSC thermograms regardless of various take-up velocities, indicating there is no distinct enhancement of thermal property by increasing take-up velocity. Fig. 4 shows the DSC thermograms of the PBAT and PBT fibers prepared at 5 km/min. In the case of PBAT, only one broad melting peak was observed at ca. 121 °C. No melting peaks corresponding to those of aliphatic homopolymer poly(butylene adipate) (PBA, ca. 56 °C) and aromatic homopolymer poly(butylene terephthalate) (PBT, ca. 227 °C) could be detected. Compared with PBA, the higher melting temperature (T_m) of PBAT would expand its applications in biodegradable field.

3.1.4. Mechanical properties

Stress–strain curves of PBAT fibers prepared at various take-up velocities are plotted in Fig. 5. With increasing take-up velocity, the initial tensile modulus and tensile strength of PBAT fibers are increased, while elongation at break is decreased. The enhancement of mechanical property of PBAT fibers is attributed to the enhanced molecular orientation as revealed by birefringence. The slightly increased crystallinity, which will be revealed in the following part (Fig. 6), would also make some contribution for the improvement of mechanical property.

For comparison, stress–strain curves of PBT fiber prepared at 5 km/min is also plotted in Fig. 5. It is interesting to note that PBAT fibers, especially prepared at low take-up velocity, may have elastic property based on their rubbery-like stress–strain curves. It exhibits low modulus, low tensile strength but high elongation at break. In addition, good recoverability of PBAT fibers was also observed in cyclic deformation test. Details on

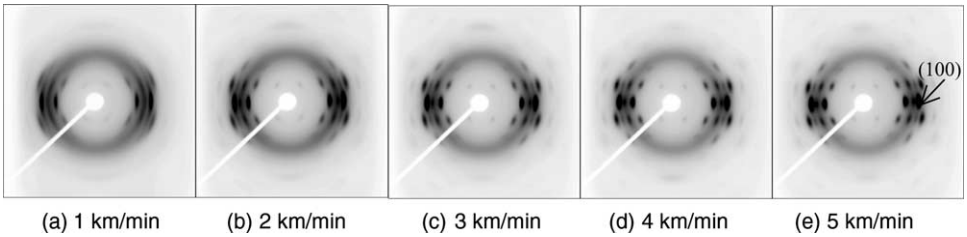

Fig. 3. WAXD patterns of PBAT fibers with take-up velocity from 1 to 5 km/min.

elastic property of PBAT fibers and its mechanism will be reported in a separate paper. In brief, the elastic property of PBAT fibers might be attributed to its chemical structure consisting of hard aromatic and soft aliphatic segments, somewhat similar to the hard and soft segmented polyurethane [24,25].

3.2. Characterization on crystal structure

3.2.1. Quantitative evaluation on crystal structure

The results of X_c, $f_{(c,z)}$ and crystallite size of (100) (see in Fig. 3) as a function of take-up velocity are plotted in Fig. 6. It suggests that the crystal structure formation of PBAT fibers was enhanced with increasing take-up velocity, although the enhancement is limited.

It is noteworthy that PBAT is an ideal random copolymer; furthermore the molar ratio of its comonomers is around 1:1. This type of copolymer has been reported to be un-crystallizable [26]. Theoretically, according to Bernoullian statistics [27], the average block length of comonomers in such kind of copolymer is close to 2, generally too short to form regular crystalline packing, or at least the crystallinity will be quite low even if it manages to crystallize. Therefore, the well-developed crystal structure in PBAT fibers is an extremely rare case, which will be further characterized below.

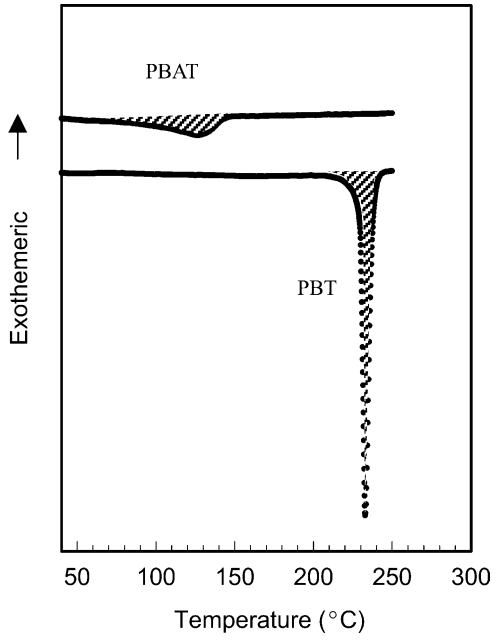

Fig. 4. DSC thermograms of PBAT and PBT fibers.

3.2.2. Characterization on WAXD pattern of PBAT

Fig. 7 shows the WAXD patterns of PBAT and PBT fibers. Similar diffraction patterns suggest that the unit cell dimensions of PBAT should be similar to that of PBT. Thus it is plausible to speculate that the crystal structure of PBAT was formed by BT unit. This view seems compatible with the crystal structure proposed for PBAT by Kuwabara et al. [18], where the crystal structure was clarified to be formed by BT unit, and BA unit is excluded from the crystalline domain.

However, it has been also reported that alternating copolymer poly(butylene terephthalate/adipate) (PTMTA) also has a closely resemble crystal lattice to that of α-form PBT crystal [28]. Table 1 shows the comparison of the observed and calculated lattice spacings (d_{obs} and d_{cal}). Spacing d_{obs} was calculated according to the angle of diffraction spots using Bragg equation; while theoretical value d_{cal} for each *hkl* plane was calculated by using crystallographic parameters of α-form PBT and PTMTA, respectively [28]. Based on the results listed in Table 1, in PBAT, the possibility that BA unit might be included in BT crystal lattice can not be excluded.

3.3. Melting temperature depression

The aforementioned analysis on the WAXD patterns of PBAT fibers failed to determine whether its crystal structure was formed by BT unit only or by both BT and BA units. Assuming it was formed by pure BT units, and then the melting

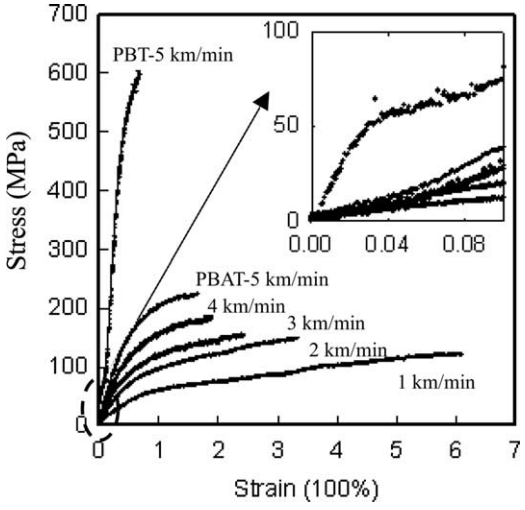

Fig. 5. Stress–strain curves of PBAT fibers and PBT fibers. Take-up velocity is as indicated.

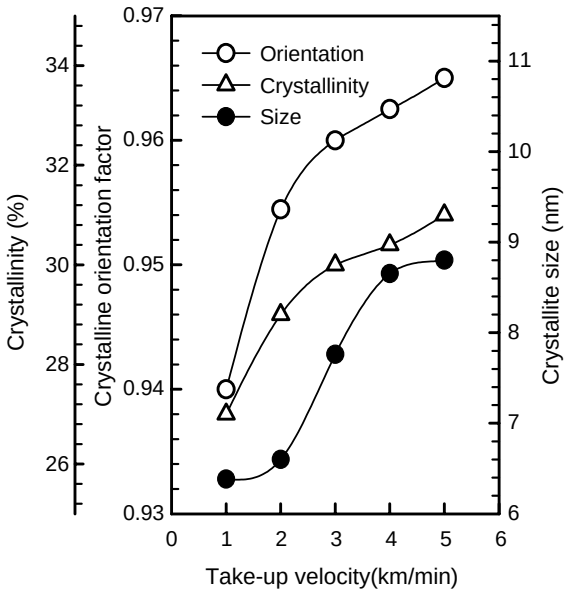

Fig. 6. Quantitative analysis results on crystal structure of PBAT fibers prepared at various take-up velocities as indicated.

temperature depression of BT crystal in PBAT is over 100 °C compared with that of PBT homopolymer as shown in Fig. 4. According to Flory [29,30], if only one kind of comonomer crystallizes in a random copolymer, the non-crystalline comonomer will hinder the crystallization process. This leads to imperfect crystallites and hence leads to melting temperature depression. The depressed melting temperature can be calculated as follows:

$$\frac{1}{T_m^0}-\frac{1}{T_m^*}=-\left(\frac{R}{\Delta H_m}\right)\ln P \tag{6}$$

where T_m^0 and T_m^* are the equilibrium melting temperatures of a random copolymer and the corresponding homopolymer of its crystallizable units, respectively. P is the molar fraction of crystallizable units, ΔH_m is the heat of fusion of the homopolymer of crystallizable units, and R is the gas constant.

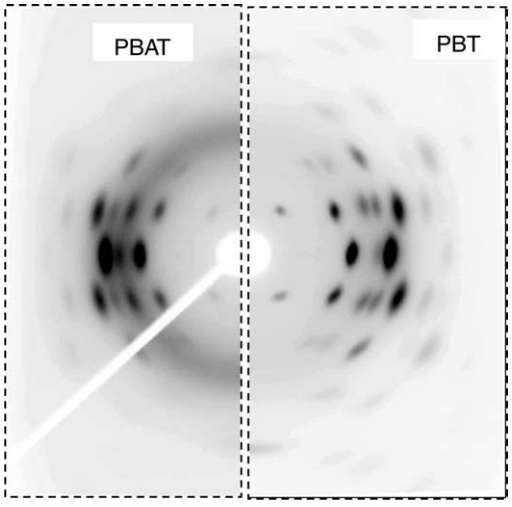

Fig. 7. Comparison of WAXD patterns of PBAT and PBT.

Table 1
Comparison of the observed and calculated lattice spacing of PBAT, α-form PBT, PTMTA

PBAT	α-form PBT		PTMTA	
d_{obs} (nm)	*hkl*	d_{cal} (nm)	*hkl*	d_{cal} (nm)
0.509	010	0.513	010	0.507
0.419	$\bar{1}10$	0.418	$\bar{1}10$	0.417
0.383	100	0.383	100	0.380
0.541	$0\bar{1}1$	0.548	$0\bar{1}2$	0.555
0.431	$\bar{1}11$	0.427	$\bar{1}12$	0.427
0.354	$1\bar{1}1$	0.352	$1\bar{1}2$	0.354

Unit cell dimensions [28], α-form PBT, *a*, 0.483 nm; *b*, 0.596 nm; *c*, 1.162 nm; α, 99.9°; β, 115.2°; γ, 111.3°; PTMTA, *a*, 0.489 nm; *b*, 0.590 nm; *c*, 2.505 nm; α, 102.3°; β, 116.8° γ, 108.8°.

In the case of PBAT, assuming that its crystal structure was formed by BT unit, the depressed equilibrium melting temperature (T_m^0) was calculated to be ca. 180 °C by applying the data of T_m^* (238 °C) [31], ΔH_m (145 J/g) [32] and P (0.44). It is much higher than the observed melting point (T_m) of 121 °C.

In addition to the observed melting temperature (T_m), further measurement on the equilibrium melting temperature (T_m^0) of PBAT was carried out using Hoffman-Weeks plot [21]. The extrapolated T_m^0 value is 128.2 °C as shown in Fig. 8, which is significantly lower than the theoretical value of 180 °C. Despite of the well-developed crystal structure, the significant melting temperature depression suggests that the crystal structure of PBAT is unlikely formed by BT units only.

3.4. Weight fraction of crystallizable BT sequences

The analysis on the weight fraction of crystallizable BT sequence in PBAT was conducted. The purpose was to estimate the maximum crystallinity of PBAT if the crystal structure is formed by BT units only.

According to Bernoullian statistics [27] and the method suggested by Yamadera [33], the average block length of BT

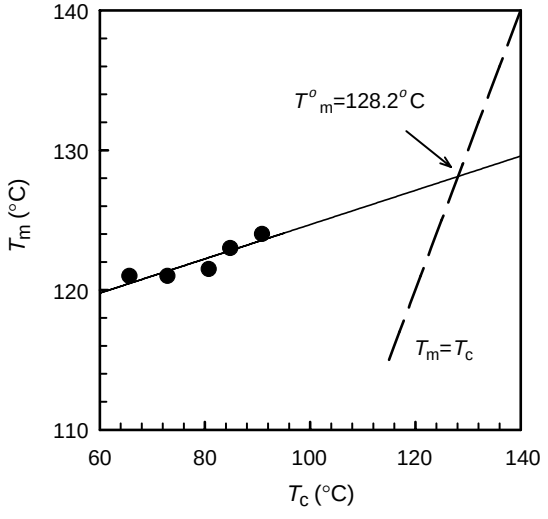

Fig. 8. Determination of the equilibrium melting temperature (T_m^0) of PBAT according to Hoffman–Weeks plot.

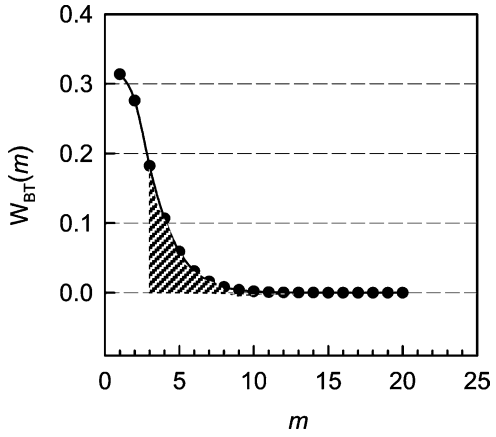

Fig. 9. The weight fraction of BT sequences as a function of m-repeating units. The shadowed part represents the sequence fractions with $m \geq 3$.

unit in PBAT is 1.8. It is no doubt that such a short BT sequences are difficult to crystallize rather than to form well-developed crystal structure. However, there should be some sequences longer than the average block length. According to random copolymer statistics [34], the number fraction ($N_x(m)$) and the weight fraction ($W_x(m)$) with sequence length of m-repeating units can be estimated using Eqs. (7) and (8), respectively.

$$N_x(m) = p^{(m-1)}(1-p) \tag{7}$$

$$w_x(m) = mP^{(m-1)}(1-P)^2 \tag{8}$$

where P represents the mole fraction of X repeating units and $m \geq 1$.

In the case of PBAT, $W_{BT}(m)$ as a function of m is plotted in Fig. 9, where P is 0.44. Assuming the sequences with the length of $m \geq 3$ are crystallizable; the weight fraction of crystallizable BT sequences was estimated to be ca. 41%. Consequently, assuming the crystal structure of PBAT is formed by BT units and considering the weight fraction of BT units (ca. 49%), its crystallinity will be lower than 20% even if all the crystallizable BT sequences are included in the crystalline region. However, the crystallinity of PBAT fibers prepared at 5 km/min is above 30% (Fig. 6). Hence, it can be excluded by sure that crystal structure of PBAT was formed by BT units only. Since this conclusion was drawn based on the assumption that the crystallizable BT sequences have repeating unit $m \geq 3$, the following analysis on crystal lamellar thickness will be given to verify this assumption.

3.5. Crystal lamellar thickness

In semi-crystalline polymers, a two-phase morphology consisting of lamella shaped crystals dispersed in an amorphous matrix is widely accepted; and quantitative details of such morphology can be estimated by small-angle X-ray scattering (SAXS), with often remarkable accuracy [35–37]. In the case of fiber, it contains regions of approximately parallel lamellae, which are oriented perpendicular to the fiber axis, and the parallel lamellae can be approximately superimposed by a shift of an identity period (long period) along the fiber axis. Based on such morphology, the minimum crystallizable sequence length can be estimated from the thickness of lamella.

Assuming the boundary of the above mentioned two phases is infinitively sharp, the lamellar thickness can be determined using one-dimensional correlation function $\gamma_1(x)$ [36].

$$\gamma_1(x) = \frac{\int_0^\infty s^2 I(s)\cos(2\pi xs)\mathrm{d}s}{\int_0^\infty s^2 I(s)\mathrm{d}s} \tag{9}$$

where, s is the magnitude of scattering vector defined by $s = 2\sin\theta/\lambda$, and I, the scattering intensity.

The one-dimensional correlation function ($\gamma_1(x)$) corresponding to the morphology of PBAT fiber prepare at 5 km/min was calculated and is shown in Fig. 10. Accordingly, the lamellar thickness (d) can be calculated using Eq. (10), provided crystallinity is below 50%.

$$d = \frac{aL - \sqrt{a^2L^2 - 4aL}}{2a} \tag{10}$$

where L is long period corresponds to the x value of the first maximum, 8.8 nm in Fig. 10; $-a$, the slope in the initial linear region of the correlation function (γ_1), -0.523 in Fig. 10. Accordingly the lamellar thickness was calculated to be 2.8 nm. In addition, crystallinity in volume fraction (X_c^v) of PBAT fibers (5 km/min) can be simply estimated to be 31.8% using values of L and d, which roughly agrees with the value of X_c (ca. 31%) revealed by WAXD.

On the other hand, the lamellar thickness can be represented by the crystallite size of the crystalline plane which is perpendicular to molecular chain orientation. In the case of PBAT fiber, as shown in Fig. 11, the lamellar thickness can be roughly estimated by the crystallite size of ($\bar{1}04$) using Scherrer

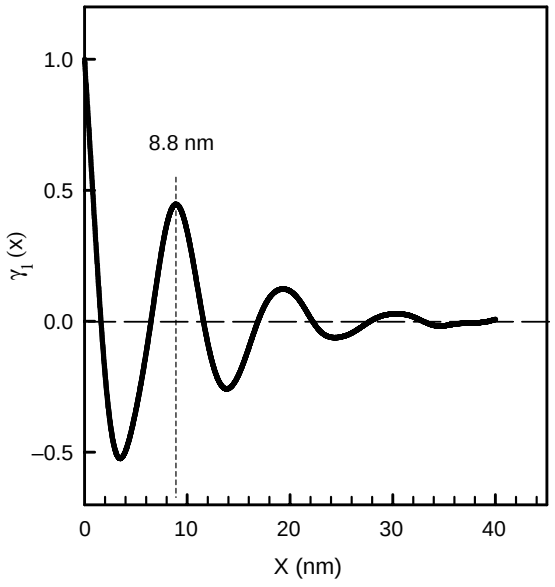

Fig. 10. Calculated one-dimensional correlation function based on PBAT fiber morphology.

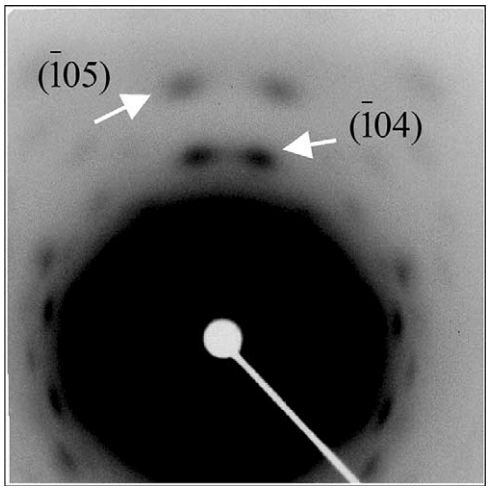

Fig. 11. WAXD pattern of PBAT fiber with sample bundle tilted to the incident X-ray beam.

equation. It gives a value of 3.2 nm. This value agrees with the result obtained from SAXS.

Since c-axis length of α-form PBT crystal lattice is 1.16 nm [28], the value of lamellar thickness of 2.8–3.2 nm in PBAT suggests that, if the crystal structure is formed by BT unit, more than 2 BT repeating units should be included in one lamella in fiber axis. This result strongly supports the assumption on BT crystallizable sequence length ($m \geq 3$).

3.6. Mixed-crystallization

Summarizing the analyses on melting temperature depression, the crystallinity and the weight fraction of crystallizable BT units, both BT and BA units are concluded to be included in crystalline region of PBAT. On the other hand, only PBT-like diffraction spots are observed in Fig. 3, and only one melting peak is observed in Fig. 4. Therefore, in PBAT fibers, BT and BA units must share a common crystal lattice by introducing the soft BA unit into BT crystal lattice. Such crystallization behavior is defined as mixed-crystallization [38–40]. A quite similar example is the crystal structure of the copolymer of hexamethylene terephthalamide and hexamethylene adipamide, where the comonomers were found to be capable of replacing each other in the crystals [41,42].

In a binary random copolymer, undergoing mixed-crystallization requires two preconditions: (1) a similar main-chain conformation between two comonomer segments in the crystal lattice, which leads to negligible geometrical hindrance when forms mixed-crystallization; (2) two comonomers should have comparable cohesive energy, otherwise, only the comonomer with larger cohesive energy will migrate to form a rich domain and be crystallized. In the case of PBAT, for the first precondition, the reported study on crystal structure of alternating copolymer PTMTA suggests that soft BA unit can adjust its chain conformation to be similar to that of BT unit [28]. And for the second precondition, the cohesive energies of BT units (E_{BT}) and BA units (E_{BA}) in PBAT were calculated using group contribution method [43]. Table 2 lists the cohesive energy value of each functional group included in PBAT, and the corresponding numbers of functional group for both BA and BT units. Using the above data and the molar ratio of BA of 56 mol% and BT of 44 mol%, the ratio of E_{BT} to E_{BA} is estimated to be 1.03. It suggests that co-crystallization is possible in PBAT in regard of dynamic stability as well. The co-crystallization is defined as that the comonomers both crystallize but not necessary to share a common lattice. The above two points strongly support the conclusion of mixed-crystal structure of PBAT fibers.

Table 2
Cohesive energy of function group and the numbers of corresponding functional group in PBAT

Function group	Cohesive energy of function group (kJ/mol)	Number of function group	
		BA	BT
$-CH_2-$	4.19	8	4
–COO–	13.41	2	2
Aromatic ring	31.00	/	1

3.7. Crystal form transition

It is well known that PBT has two crystal forms (α and β), which are reversible to each other by tensile deformation and relaxation [44–47]. In the case of PBAT, in which soft BA unit is introduced into BT crystal lattice, interest was aroused to investigate whether such mixed-crystal structure also undergoes PBT-like crystal form transition. Therefore, in situ WAXD measurement during tensile deformation on PBAT fibers was conducted. PBT fibers were used as reference.

In the case of PBT, the most characteristic crystallographic reflections in WAXD pattern are (1̄04) at 31.4° and (1̄05) at 39.5° for the α-form as shown in Fig. 12(a); and are (1̄04) at 28.2° and (1̄06) at 43° for the β-form as shown in Fig. 12(c), respectively. Fig. 12(b) shows the coexistence of α and β forms. These characteristic reflections are generally used to judge the crystal form of PBT [46]. Fig. 12(d)–(f) shows the WAXD patterns of PBAT fiber recorded under the tensile strain as indicated. Diffraction spots corresponding to (1̄04) at 30.8° and (1̄05) at 39.5° of α-form PBT crystal were clearly observed in Fig. 12(d) when PBAT fiber was in the relaxed state. This is strong evidence again that PBAT has a similar crystal lattice to that of α-form PBT. When PBAT fiber was stretched to 43% (Fig. 12(e)), new diffraction spots at 42.8° corresponding to (1̄06) of β-form PBT crystal was observed. With the further tensile deformation, this β-form diffraction became dominated in Fig. 12(f). More detailed crystal form changes in PBAT fibers, revealed by meridional intensity profiles during tensile deformation and after relaxation are shown in Fig. 13. With the increase of tensile deformation, peaks assigned to α-form became weak, while the peak assigned to β-form became more distinct and at last became dominated when tensile strain was above 63%. Further more,

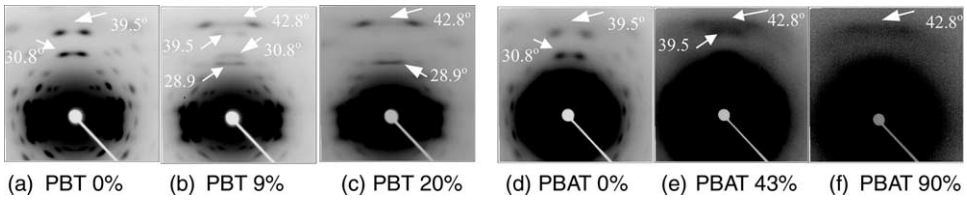

Fig. 12. WAXD patterns of PBT and PBAT fibers recorded during tensile deformation.

β-form reversed to α-form when sample was relaxed as shown in Fig. 13(g). Summarizing the above, it is interesting to find that mixed-crystal structure of BT and BA units also undergoes PBT-like crystal form transition with the application or removal of the tensile stress. It is noteworthy that, in the case of PBT, α-form totally transforms into β-form when tensile strain is over 15% [47]. However, in the case of PBAT, α-form remains dominated even at the tensile strain of 17% as shown in Fig. 13(b). Such discrepancy might be due to the much lower modulus of PBAT fibers compared with that of PBT fibers as showed in Fig. 5. Since the crystal form transition in PBT has been reported to occur above a critical stress (ca. 75 MPa at room temperature) [45], most likely similar precondition is also required in the case of PBAT. Consequently, PBAT fibers require a higher strain to reach this critical stress.

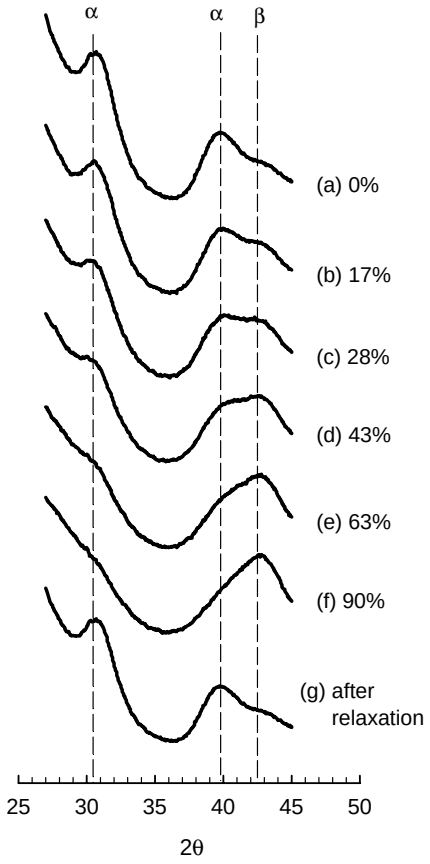

Fig. 13. Meridional diffraction intensity profiles of PBAT fibers during tensile deformation and after relaxation.

4. Conclusions

PBAT copolymer showed good spinnability in melt-spinning process. The attainable highest take-up velocity was 5 km/min. Higher take-up velocity led to the enhancement in molecular orientation, crystal structure and mechanical properties of PBAT fibers, but no distinct effect on thermal property.

The crystal structure of PBAT fibers was characterized to be formed by mixed-crystallization of BT and BA units. Mixed crystallization enabled PBAT to have well-developed PBT-like crystal structure despite of its ideal randomness and (1:1) composition. The introduction of soft BA unit into BT crystal lattice led to the significant lower melting temperature compared with that of PBT.

It is interesting to find that the mixed-crystal structure of PBAT fibers also undergoes PBT-like reversible crystal forms transition. However, due to the elastic property of PBAT fibers, α to β form transition was found to occur in a higher strain region compared with that of PBT fibers.

References

[1] Doi Y. Microbial polyesters. New York: VCH Publisher; 1990.
[2] Lenz RW. Adv Polym Sci 1993;107:1.
[3] Doi Y, Fukuda K, editors. Biodegradable plastics and polymers. Amsterdam: Elsevier; 1994.
[4] Amass W, Amass A, Tighe B. Polym Int 1998;47:89.
[5] Sudesh K, Abe H, Doi Y. Prog Polym Sci 2000;25:1503.
[6] Chiellini E, Solaro R, editors. Macromolecular symposium; 2003, 2003. p. 197.
[7] Scott G. Polym Degrad Stab 2000;68:1.
[8] Okada M. Prog Polym Sci 2002;27:87.
[9] Maeda Y, Maeda T, Yamaguchi K, Kubota S, Nakayama A, Kawasaki N, et al. J Polym Sci, Part A: Polym Chem 2000;38:4478.
[10] Jin HJ, Lee BY, Kim MN, Yoon JS. Eur Polym J 2000;36:2693.
[11] Rantze E, Kleeberg I, Witt U, Müller RJ, Deckwer WD. Maromol Symp 1998;130:319.
[12] Yoo ES, Im SS. Macromol Symp 1997;118:739.
[13] Witt U, Müller RJ, Deckwer WD. Maromol Chem Phys 1996;197:1525.
[14] Uwe W, Rolf-Joachim M, Wolf-Dieter D. J Environ Polym Degrad 1995; 3(4):215.
[15] Ki HC, Park OOk. Polymer 2001;42:1849.
[16] Müller RJ, Kleeberg I, Deckwer WD. J Biotechnol 2001;86:87.
[17] Witt U, Müller RJ, Deckwer WD. J Environ Polym Degrad 1997;5(2):81.
[18] Kuwabara K, Gan Z, Nakamura T, Abe H, Doi Y. Biomacromolecules 2002;3:390.
[19] Cranston E, Kawada J, Raymond S, Morin FG, Marchessault RH. Biomacromolecules 2003;4:995.
[20] Shi XQ, Aimi K, Ito H, Ando S, Kikutani K. Polymer 2005;46:751.
[21] Hoffman JD, Weeks JJJ. J Res Natl Bur Std (US) 1962;66(A):13.
[22] Hermans JJ, Hermans PH, Vermeas D, Weidinger A. Recl Chim Trav 1946;65:427.
[23] Scherrer P. Göettinger Nachr 1918;2:98.

[24] Wang CB, Cooper SL. Macromolecules 1983;16:775.
[25] Kimura I, Ishihara H, Ono H, Yoshihara N, Nomura S, Kawai H. Macromolecules 1974;7(3):355.
[26] Kang HJ, Park SS. J Appl Polym Sci 1999;72:593.
[27] Bovey FA, Tiers GVD. J Polym Sci 1960;44:173.
[28] Atfani M, Brisse F. Macromolecules 1999;32:7741.
[29] Flory PJ. Trans Faraday Soc 1955;51:848.
[30] Marrs W, Peters RH, Still RH. J Appl Polym Sci 1979;23:1077.
[31] Chishholm BJ, Zimmer JG. GE Research and Development Center, 2000CRD002, March 2000.
[32] Wunderlich B. Macromolecular physics. vol. 2 and 3. New York: Academic press; 1980 p. 1976.
[33] Yamadera R, Murano M. J Polym Sci 1967;5:2259.
[34] Coleman BD, Fox TG. J Polym Sci 1963;part A-1:3183.
[35] Jenkins AD, Baltá-Calleja FJ, Vonk CG. X-ray scattering of synthetic polymers. Amsterdem: Elsevier; 1989 [Chapter 7].
[36] Glatter O, Kratky O. Small angle X-ray scattering. New York: Academic press; 1982.
[37] Dawkins JV. Developments in polymer characterization-1. London: Applied Science; 1978 [Chapter 6].
[38] Bluhm TL, Hamer GK, Marchessault RH, Fyfe CA, Veregin RP. Macromolecules 1986;19:2871.
[39] Helfand E, Lauritzen JI. Macromolecules 1973;6(4):631.
[40] Wunderich B. Macromolecular physics. vol. 1. New York: Academic Press; 1973 [Chapter 2–4].
[41] Edgar OB, Hill R. J Polym Sci 1952;8:1.
[42] Billmeyer Jr FW. Textbook on polymer science. 2nd ed. New York: Wiley; 1962 [Chapter 7].
[43] Van Krevelen DW. Properties of polymers. Amsterdam: Elsevier; 1990 [Chapter 7].
[44] Al-jishi R, Taylor PL. Macromolecules 1988;21:2240.
[45] Carr Pl, Jakeways R, Klein JL, Ward IM. J Polym Sci 1997;35:2465.
[46] Yokouchi M, Sakakibara Y, Chatani Y, Tadokoro H, Tanaka T, Yoda K. Macromolecules 1976;9(2):266.
[47] Tashiro K, Nakai Y, Kabayashi M, Tadokoro H. Macromolecules 1980; 13:137.